Received: 31 January 2019 | Revised: 11 June 2019 | Accepted: 1 July 2019

DOI: 10.1002/elsc.201900021

Engineering in Life Sciences

RESEARCH ARTICLE

Inulinase immobilization on polyethylene glycol/polypyrrole multiwall carbon nanotubes producing a catalyst with enhanced thermal and operational stability

Mishela Temkov[1,6] | Aleksandar Petrovski[1] | Emilija Gjorgieva[2] | Emil Popovski[2] | Maja Lazarova[3] | Ivan Boev[3] | Perica Paunovic[1] | Anita Grozdanov[1] | Aleksandar Dimitrov[1] | Aliaksandr Baidak[4,5] | Albert Krastanov[6]

[1]Faculty of Technology and Metallurgy, Ss. Cyril and Methodius University in Skopje, Skopje, Republic of Macedonia

[2]Institute of Chemistry, Faculty of Natural Science and Mathematics, Ss. Cyril and Methodius University in Skopje, Skopje, Republic of Macedonia

[3]Technological Technical Faculty, University Goce Delcev, Shtip, Republic of Macedonia

[4]Dalton Cumbrian Facility, University of Manchester, West Lakes, United Kingdom

[5]School of Chemistry, University of Manchester, Manchester, United Kingdom

[6]Faculty of Technology, University of Food Technologies, Plovdiv, Bulgaria

Correspondence
Mishela Temkov, Department of Food Technology and Biotechnology, Faculty of Technology and Metallurgy, Ss. Cyril and Methodius University in Skopje, Rudjer Boskovic 16, 1000 Skopje, Republic of Macedonia.
Email: mishela@tmf.ukim.edu.mk

Funding information
Bulgarian National Science Fund

This paper describes the development of a simple method for mixed non-covalent and covalent bonding of partially purified inulinase on functionalized multiwall carbon nanotubes (*f*-MWCNTs) with polypyrrole (PPy). The pyrrole (Py) was electrochemically polymerized on MWCNTs in order to fabricate MWCNTs/PPy nanocomposite. Two multiple forms of enzyme were bound to N-H functional groups from PPy and -COO^- from activated MWCNTs to yield a stable MWCNTs/PPy/PEG immobilized preparation with increased thermal stability. Fourier transform infrared (FTIR) spectroscopy and scanning electron microscopy (SEM) were used to confirm functionalization of nanoparticles and immobilization of the enzyme. The immobilization yield of 85% and optimal enzyme load of 345 μg protein onto MWCNTs was obtained. The optimum reaction conditions and kinetic parameters were established using the UV-Vis analytical assay. The best functional performance for prepared heterogeneous catalyst has been observed at pH 3.6 and 10, and at the temperatures of 60 and 80ºC. The half-life ($t_{1/2}$) of the immobilized inulinase at 60 and 80ºC was found to be 231 and 99 min, respectively. The reusability of the immobilized formulation was evaluated based on a method in which the enzyme retained 50% of its initial activity, which occurred after the eighteenth operation cycle.

KEYWORDS
enzyme immobilization, functionalization, inulinase, multiwalled carbon nanotubes, polyethylene glycol, polypyrrole

1 | INTRODUCTION

Inulin is homobiopolymer formed of linear chains of β 2,1-D-fructofuranose molecules terminated with a glucose residue at the position β 1,2. Inulinases (2,1-β-D-fructan fructanohydrolase, EC 3.2.1.7) are the enzymes that hydrolyze inulin, producing fructooligosaccharides, fructose, and glucose as main products [1]. Fructooligosaccharides can be employed as functional ingredients in food products, acting as prebiotics, sugar substitutes, or fat replacers [2]. Inulinases are versatile biocatalysts extensively used in a wide range of industrial processes for obtaining high fructose syrup [3–5] and fructooligosacharides [6,7], and to a lesser extent,

Abbreviations: ATPS, aqueous-two phase system; CNT, carbon nanotube; *f*-MWCNT, functionalized multiwall carbon nanotube; FTIR, Fourier transform infrared; $t_{1/2}$, half-life; MWCNT, multiwall carbon nanotube; PPy, polypyrrole; Py, pyrrole; SEM, scanning electron microscopy.

bioethanol [8,9], citric acid [10], alcohols and lactic acid [11]. However, using the enzymes in their free form is not economically viable due to their structural instability and the loss of the enzyme during hydrolysis; moreover, released inulinase might also contaminate the products of reaction [12]. Immobilization, i.e. the loading of an enzyme onto supporting template, can be used to overcome these limitations. Immobilization simplifies enzyme handling, provides easier separation of the catalyst from the product; it mitigates the contamination of a final product, and allows for efficient recovery of the enzyme and its repeated use [13,14]. Another benefit of immobilization is the improved structural stability of an enzymatic system towards heat and organic solvents, as well as increased resistance to autolysis [14]. Immobilized enzymes exhibit enhanced operational stability, therefore, represent more preferred choice for continuous automated processes in comparison to free enzyme forms [12]. The choice of carrier is determined by the cost of the catalyst that should not exceed a few percent of the total production cost [15].

Previously, inulinase has been immobilized on various supports, e.g. biopolymers (chitin, chitosan, alginate) [16–20], synthetic polymers (polyurethane foam, polyvinyl alcohol) [21,22], inorganic supports (MWCNT, silica nanoparticles) [3,23–25], or hybrids consisting of organic and inorganic parts (poly-d-lysine coated $CaCO_3$ microparticles, magnetic nanoparticles with wheat gluten hydrolysates, magnetite chitosan microparticles) [26–28]. Generally speaking, nanomaterials are currently widely used for immobilization of proteins. Particular examples include, but are not limited to, enzymes, gene delivery, and fabrication of various drugs and vaccines as well as in cancer therapy [29].

Wide use of nanomaterials for immobilization is due to their extraordinary properties, such as mass transfer resistance and high specific surface area, both favor significant loading of biomolecules onto a matrix [30–33]. Among nanomaterials, carbon nanostructures have attracted great attention for potential applications in biotechnology [24,30,34–37].

CNTs are folded graphene layers in form of a cylinder with diameter of several nanometers and length of few micrometers [31,36,38,39]. CNTs in their pristine form do not possess any functional groups. Nevertheless, their surface can be easily modified by: (a) partial oxidation of carbon nanomaterials resulting in creation of various oxygen-containing functionalities within its structure; (b) non-covalent as well as (c) covalent functionalization [38]. Upon functionalization of CNTs, their dispersibility in suitable solvents increases while their tendency to aggregate reduces. Functionalization is known to enhance interactions of modified CNTs with biomolecules afforded through van der Waals forces, hydrogen or covalent bonding [40,41]. The electrical conductivity and mechanical properties of composite materials can be enhanced if CNTs are introduced into a conductive polymer such as PPy. This polymer is easily synthesized and has good stability under ambient conditions [42]. The nanocomposite consisting of CNT and PPy or PEG has been shown to penetrate mouse B-cells cortical neurons with only 10% non-viable cells [43]. This finding has inspired further research into using the CNT/PPy composite as a carrier for targeted drug delivery [44].

Using CNTs for immobilization of enzymes is another promising research area. For example, Mubarak et al., 2014 [30] have reported successful non-covalent immobilization of cellulase onto functionalized CNTs by oxidation featuring high enzyme loading and prolonged reusability of the immobilized preparation. Pavlidis et al., 2010 [35] reported the immobilization of *Candida antarctica* lipase B on MWCNTs, which were covalently functionalized by tetra-n-octylammonium bromide and hexadecylbromide. Kim et al., 2009 [36] have shown successfully achieved immobilization of HRP on MWCNTs using succinimidyl ester as a cross-linker; while Garlet et al., 2014 [24] have used the oxidized MWCNTs containing carboxylic groups (-COOH) for non-covalent inulinase immobilization and reported very fast and highly efficient adsorption of the enzyme into immobilized formulation. On contrary, Kim et al. [45] reported a simple immobilization of glucose oxidase on intact MWCNTs by adding them directly into an aqueous enzyme solution, resulting in simultaneous CNT dispersion and facile enzyme immobilization through sequential enzyme adsorption, precipitation, and crosslinking by glutaraldehyde. In more recent study, Singh et al. [3] used modified MWCNTs with 3-aminopropyl-triethoxysilane to generate amino-terminated surfaces for inulinase from *Penicillium oxalicum* immobilization and obtained maximal inulinase activity of 60.7% and immobilization yield of 74.4%, while the enzyme lost 28% of its initial activity after the tenth

PRACTICAL APPLICATION

This work concerns the development of a new in situ method for a mixed (physical and chemical) immobilization of inulinase onto the carbon-polymer nanocomposite. More specifically, inulinase (an enzyme that hydrolyses inulin into fructooligosaccharides), sourced from Bacillus sp. 11/3, has been immobilized onto activated multiwalled carbon nanotubes/polypyrrole (MWCNT/PPy) composite. Prior to immobilization, the enzyme was partially purified in PEG phase by a technique called aqueous two-phase systems (ATPSs). The main advantage of our approach is that it allows skipping the separation of the enzyme from the PEG phase and hence provides a straightforward method for direct inulinase immobilization onto MWCNTs.

cycle. Later, in another study, the same author Sing at al. [23] immobilized the same inulinase on aminated MWCNTs by glutaraldehyde cross-linking process and reported increased inulinase activity of 1.22-fold and increased immobilization yield of 1.14-fold, in comparison to his previous study.

In this work, a successful use of carbon nanomaterials for a novel method of inulinase immobilization is demonstrated. Inulinase was produced by submerged fermentation of *Bacillus* sp. 11/3, as described in Temkov et al. [46]. The enzyme was partially purified by ATPS and then immobilized onto MWCNTs. The inulinase was extracted in PEG phase. The novelty of our approach is the one-step straightforward fabrication of immobilized preparation. Namely, after the extraction of the inulinase in the PEG phase, the separation of the enzyme, which is commonly performed by using time-consuming ultrafiltration, can be skipped and the catalyst can be prepared directly from PEG, producing a preparation with enhanced thermal and operational stability.

According to the literature, the adsorption of PEG on the PPy stabilizes the particles and occurs probably via hydrogen bonding mechanism with the pyrrole (Py) N-H group [47]. PEG derivatives can be irreversibly adsorbed on carbon nanotubes (CNTs). The resulting PEG coated nanotubes can exhibit certain degree of protein resistance for nonspecific adsorption. The attachment of a protein on sidewalls of MWCNT depends on the uniformity of the polymer layer adsorbed on nanotubes. It is found that relatively small proteins (~60 kDa) can be adsorbed more readily to the sidewalls of MWCNTs [47–49]. In another study, the non-aromatic polymers have been reported to disperse CNTs via wrapping mechanism, pointing out the importance of the CH–π interaction between the polymer and the CNTs. Moreover, the hydrophobic part of the proteins connects with CNTs by multi-point OH–π interactions [50].

Our method is based on a simple physical adsorption of PEG onto functionalized multiwall carbon nanotubes (*f*-MWCNTs) assisted by the hydrogen bonding involving the N-H groups from PPy and the O-H groups from PEG. However, the enzyme seems to be attached to the nanocomposite's structure by a combination of non-covalent and covalent mechanisms. Systematic characterization of the immobilized preparation was performed in order to determine the optimal enzyme loading as well as the optimal working parameters, kinetics, and the operational stability.

2 | MATERIALS AND METHODS

2.1 | Materials

Pyrrole and SDS were supplied by Sigma Aldrich, USA. PEG (M_w = 1000 g/mol) was provided by Merck, Germany. Chemically modified MWCNTs (functionalization with –COOH groups) were received from Joint Research Centre (JRC), NM 400. Inulin isolated from the Jerusalem artichoke (degree of polymerization > 25) was a gift from Beneo, Belgium. Bradford reagent and BSA were obtained from Bio-Rad, USA. 4-Hydroxybenzhydrazide (PAH-BAH) was purchased from Alfa Aesar, Germany. All chemicals were of analytical grade. Extracellular inulinase used in these experiments was obtained by submerged cultivation from *Bacillus sp.* 11/3. All chemicals were used as received with exception of Py, which was purified by distillation prior to use.

2.2 | Electropolymerization of MWCNTs/PPy

Functionalized MWCNTs were coated with PPy by electrochemical polymerization. The electro-polymerization was performed in 100 mL three-electrode one-compartment glass cell. The working and counter electrodes were platinum tiles with active surface of 10 cm^2. Saturated calomel electrode was used as reference electrode. The polymerization electrolyte was prepared using multistep procedure. First, 0.01 M of SDS was dissolved in water. Py was added to the prepared SDS solution to achieve 0.1 M concentration of Py in the final solution. Finally, the chemically modified MWCNTs were added to the mixture. The mass ratio of *f*-MWCNTs vs. Py was kept at 1:10. Before the start of electropolymerization, the electrolyte containing carbon nanostructures was ultrasonicated for 15 min in order to obtain stable dispersion. The electrochemical polymerization of MWCNTs/PPy nanocomposite was performed at galvanostatic conditions using constant current of 2.91 mA for 15 min in order to maintain constant deposition rate [51]. For these experiments, WENKING HC 500 potentiostat/galvanostat was employed. After electro deposition, the nanocomposite was removed from the platinum electrode, washed several times with distilled water, and dried at room temperature.

2.3 | Inulinase production

Extracellular inulinase was obtained by submerged cultivation of *Bacillus sp* 11/3 isolated in the University of Food Technologies in Plovdiv. The medium used for strain isolation, maintenance, and enzyme production had the following composition (g/L): inulin, 4; yeast extract, 4; peptone, 4; $MgSO_4$, 0.16; K_2HPO_4, 0.8. The pH was adjusted to 8 with 20 wt% $NaCO_3$ aqueous solution. The fermentation was conducted in flasks placed on a moving rotary shaker (200 rpm) at 50°C for 24 h [52]. Then the culture medium was centrifuged at 14 000 rpm for 3 min to ensure total removal of the microbial cells. The supernatant was collected and stored at –18°C until further analysis. The obtained culture medium free of cells was used as a crude enzyme solution.

For the enzyme purification, the ATPS technique was used as described in our previous study [52]. The optimal system

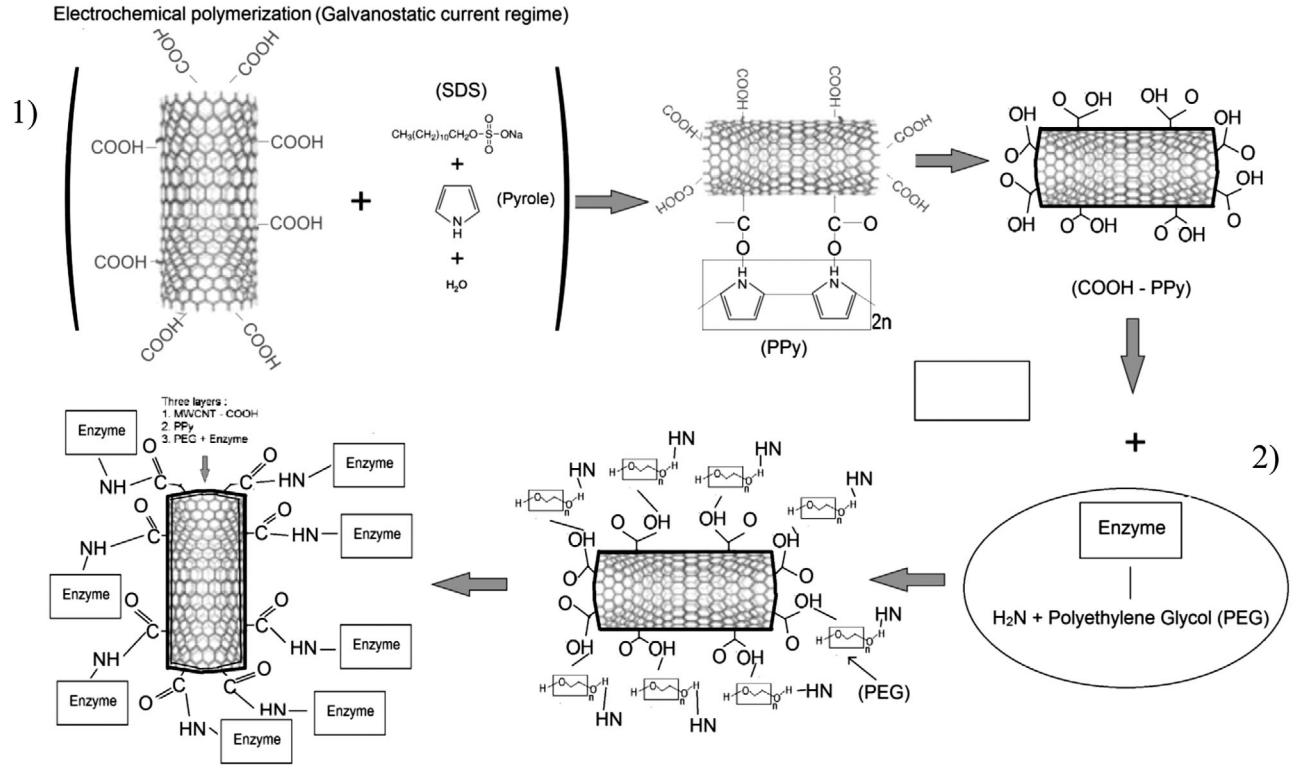

FIGURE 1 (1) Procedure of functionalization of MWCNT with PPy by electrochemical polymerization at galvanostatic conditions. First, Py was added to the prepared SDS solution, and after chemically modified MWCNTs was added to the mixture in mass ratio of *f*-MWCNTs vs. Py at 1:10 and immobilization of enzyme on *f*-MWCNT. (2) Procedure of immobilization of inulinase enzyme on functionalized MWCNTs, using concentrated PEG phase enriched with the enzyme

composition which yielded the best purification parameters, was found to be 26 wt% PEG (molecular weight 1000 g/mol) and 26 wt% $MgSO_4$. The enzyme was partitioned in PEG phase, while the bulk proteins partitioned in the salt phase. PEG phase with the entrapped enzyme was subjected to vacuum evaporation at 40°C to achieve protein concentration of 115 μg/mL in the final solution.

2.4 | Immobilization of inulinase enzyme on functionalized MWCNTs

Immobilization of inulinase onto modified *f*-MWCNTs was performed using different quantities of concentrated PEG phase enriched with the enzyme, added to 20 mg of *f*-MWCNTs. The prepared dispersions were mixed in glass tubes on a 3D shaker at 25°C, 60 rpm for 24 h, following centrifugation at 6000 rpm for 15 min. Finally, *f*-MWCNT/PPy/PEG-inulinase composites were washed four times with water to remove unbound proteins, and then left to air dry for 48 h prior to further tests. The bound protein was determined indirectly by subtracting the amount of introduced protein to the carriers and the protein recovered in the supernatant fractions. Protein concentration was determined according to Bradford method [53], using BSA as a standard. The mass ratio of immobilized inulinase on the particles represents the enzyme loading capacity. The whole procedure of fabrication of MWCNT/PPy composite and inulinase immobilization onto it is presented in Figure 1.

2.5 | Characterization of functionalized MWCNT and immobilized inulinase

The morphology of pristine MWCNTs, functionalized MWCNTs, and MWCNT/PPy/PEG-inulinase composites was determined by scanning electron microscopy (SEM) using TESCAN VEGA3LMU, equipped with the EDS analyzer from Oxford Instruments. Small samples of air dried pristine MWCNT, MWCNT/PPy, and MWCNT/PPy/PEG-enzyme composites were mounted on carbon tape on a copper stub, followed by 60 nm of gold deposition using a sputter coater. Vibrations of characteristic functional groups in these materials were characterized by Fourier transform infrared (FTIR) spectroscopy using Perkin Elmer PARAGON instrument. FTIR spectra were recorded using attenuated total reflectance technique in the frequency range of 4000 to 550 cm^{-1}, with 32 scans per minute using He-Ne laser.

2.6 | Inulinase activity assay

Inulinase activity assay was performed by incubating 0.025 g MWCNT/PPy/PEG-inulinase with 2.5 mL 2% w/v inulin

dissolved in carbonate-bicarbonate buffers (CO_3^{2-}/HCO_3^-) (pH 10) at 50°C for 20 min. After incubation, the reaction tubes were kept in a boiling water bath for 15 min to suppress the activity of inulinase and to stop the reaction; the dispersions were then cooled to room temperature. The reaction mixture was assayed for reducing sugar by a modified method described by Lever, 1972 [54]. 250 μL of the reaction mixture and 1750 μL solution of PAH BAH dissolved in 10% 0.5 M HCl and 90% 0.5 M NaOH was boiled for 10 min. After cooling, the absorbance at 410 nm was measured by using a microplate reader SPECTROSTAR–Nano (BMG LABTECH). The absorbance values were translated into the amounts of fructose produced during the reaction using a fructose calibration curve. One unit of enzymatic activity was defined as the amount of enzyme needed to liberate 1 μmol of fructose per minute under the assay conditions. Assays were performed in triplicate and average value was used in calculations. The efficiency of immobilization at different enzyme dosages was calculated by using equations (1) and (2) for the immobilization yield of protein and activity recovery, respectively:

$$\text{Immobilization yield of protein}(\%) = \left(1 - \frac{\text{Protein concentration in supernatant}}{\text{Protein concentration in PEG phase}}\right) \times 100 \quad (1)$$

$$\text{Activity recovery}(\%) = \frac{\text{Total activity of immobilized enzyme}}{\text{Total activity of enzyme in PEG phase}} \times 100 \quad (2)$$

2.7 | Operational and storage stability of immobilized inulinase enzyme

The operational stability of the immobilized enzyme was examined under the optimal conditions defined in Sections 2.8 and 2.9 and by using the enzymatic assay described in Section 2.6. The MWCNT/PPy/PEG-inulinase composite was removed by centrifugation (6000 rpm, 15 min) after each cycle, washed with distilled water, and re-suspended in new portion of 2% inulin solution for the next cycle. Each cycle lasted for 1 h, after which an aliquot of the solution was taken for the enzyme activity analysis. The activity of the immobilized enzyme after the first cycle was set as a control and assumed to possess a relative activity of 100% [30]. The aliquots of prepared catalyst were stored at 4ºC and the residual activity was determined after 6 months of storage.

2.8 | Effect of pH on immobilized inulinase activity and stability

Inulinase activity was measured at different pH in the range between 3.6–10.7 by deploying the enzyme activity assay described in Section 2.6. Acetate (CH_3COO^-/CH_3COONa) in the pH range 3.6–5.2, phosphate ($H_2PO_4^-/HPO_4^{2-}$) in the pH range 5.8–8.0, and carbonate-bicarbonate buffers (H_2CO_3/HCO_3^-) having pH from 9.5 to 10.7 were used to achieve desired pH conditions. The pH stability of free vs. immobilized inulinase was tested by preincubating free and immobilized enzyme for 120 min at 50°C in the buffer solutions with the same ionic concentrations and pH values from 3.6 to 10.7. After the incubation, the residual inulinase activity was measured under standard assay conditions. The recovered activity was normalized taking into account the same amount of enzyme for both free and immobilized form.

2.9 | Effect of temperature on immobilized inulinase activity and stability

Inulinase activity was measured in a wide temperature range between 20 and 90°C, with the measurements taken at 10°C increments, following the method described in the Section 2.6 and using the optimal pH conditions determined as described in the Section 2.8. The temperature stability of the free and immobilized enzyme was tested by preincubation in a temperature range of 20–90°C for 120 min. After the incubation, the residual inulinase activity was measured at standard assay conditions. The recovered activity was normalized taking into account the same amount of enzyme. The activity was also measured during preincubation at appropriate time intervals in order to estimate the thermal stability of the enzyme [26]. The inactivation process follows the first order reaction kinetics; it is determined according to the equation (3). The half-lives ($t_{1/2}$) and D values of the enzyme were calculated using the equations (4) and (5).

$$\ln \frac{A_0}{A} = k_d \cdot t \quad (3)$$

$$t_{1/2} = \frac{\ln 2}{k_d} \quad (4)$$

$$\text{D value} = \frac{\ln 10}{k_d} \quad (5)$$

where A_0 and A are the initial and the residual activities, respectively, and k_d represents the inactivation rate constant.

2.10 | Kinetic studies

To obtain kinetic parameters, K_m and V_{max} for inulinase, 5 mL aliquots containing 0.5, 1.0, 1.5, 2.0, 2.5, and 3.0% of

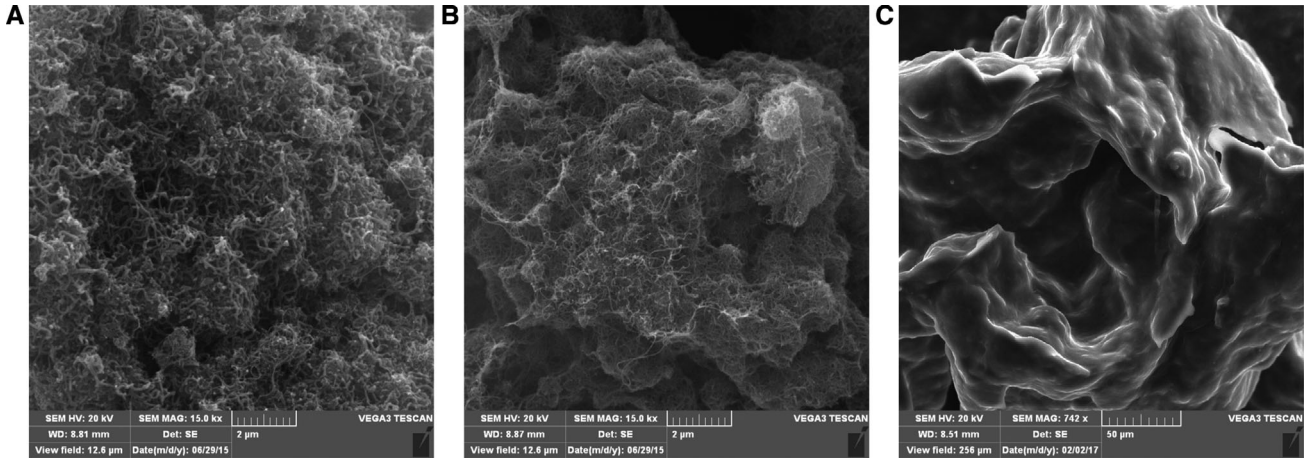

FIGURE 2 SEM images of: (A) pristine *f*-MWCNTs with -COOH functionalization, which exhibits a presence of defects manifesting themselves as irregularities in shape or as agglomeration of the CNTs; (B) MWCNTs/PPy nanocomposite, which exhibits globular morphology featuring CNTs wrapped with polymer sheets of PPy; and (C) MWCNTs/PPy/PEG-inulinase catalyst, which becomes completely wrapped with PEG-inulinase

inulin were hydrolyzed with 0.025 g of the immobilized inulinase in 0.1 M carbonate-bicarbonate buffer (H_2CO_3/HCO_3^-) (pH 10) at 30°C for 20 min. The reaction was terminated at 100°C for 15 min. A Lineweaver–Burk plot was generated to obtain the K_m and V_{max}, and the values were expressed as the mean of the triplicate experiments.

3 | RESULTS AND DISCUSSION

3.1 | Characterization of functionalized MWCNTs/PPy and MWCNTs/PPy/PEG-enzyme composites

3.1.1 | SEM

SEM was used to explore the changes in morphology of the MWCNTs upon formation of its nanocomposites with PPy and PEG–inulinase. Three systems were characterized, namely: (1) pristine *f*-MWCNTs with -COOH functionalization, (2) MWCNTs/PPy nanocomposite and (3) MWCNTs/PPy/PEG-inulinase catalyst. Obtained SEM images of these materials are shown in Figures 2A, 2B, and 2C, respectively. As can be seen from Figure 2A, the morphology of pristine *f*-MWCNTs is represented by bundles of intertwined nanotubes with a length of several micrometers. Some regions of *f*-MWCNTs exhibit defects manifesting themselves as irregularities in shape or as agglomeration of the CNTs. The appearance of these defects can be attributed to the chemical modification of this material. Figure 2A also shows that *f*-MWCNTs have porous structure. The pores, uneven sites, and other defected regions are preferred locations for functionalization; hence, this is where carboxylic groups are likely to be formed [55]. The morphology of the nanocomposite consisting of COOH-MWCNTs and PPy is shown in Figure 2B. As can be seen in this SEM image, the original porosity of COOH-MWCNTs is reduced due to the PPy filling in void spaces between CNTs. The formed nanocomposite of COOH-MWCNTs and PPy exhibits globular morphology featuring CNTs wrapped with polymer sheets of PPy. Although reduced in comparison to pristine f-MWCNTs, the remaining porosity of the *f*-MWCNTs/PPy nanocomposite is beneficial for the formation of the target *f*-MWCNTs/PPy/PEG-inulinase nanocomposite. The SEM image for the latter, shown in Figure 2C demonstrates that the *f*-MWCNTs/PPy material becomes completely wrapped with PEG-inulinase in the final nanocomposite. This type of morphology reflects the formation of much larger structures with the size up to 100 μm, in which pores become hidden or filled in comparison to the *f*-MWCNT and the *f*-MWCNTs/PPy composites. This result suggests that the enzyme becomes completely entrapped within the nanocomposite structure, i.e. the desired loading of the inulinase onto the matrix is successfully accomplished.

3.1.2 | FTIR Spectroscopy

In order to determine which chemical bonds were affected by the synthetic modifications, all materials of interest were investigated using FTIR spectroscopy in attenuated total reflectance mode. In Figure 3A, FTIR spectra of the pristine *f*-MWCNTs and *f*-MWCNT/PPy nanocomposite are shown. Pristine *f*-MWCNTs as well as the *f*-MWCNTs/PPy nanocomposite (Figure 3A) give featureless infrared spectra with just a handful of characteristic peaks, which is in accord with the previously published data [56]. The bands appearing at 1652 cm^{-1} and in the region of 1512 to 1567 cm^{-1} of the *f*-MWCNTs sample correspond to the asymmetric and symmetric stretching of the aromatic rings [57]. Furthermore,

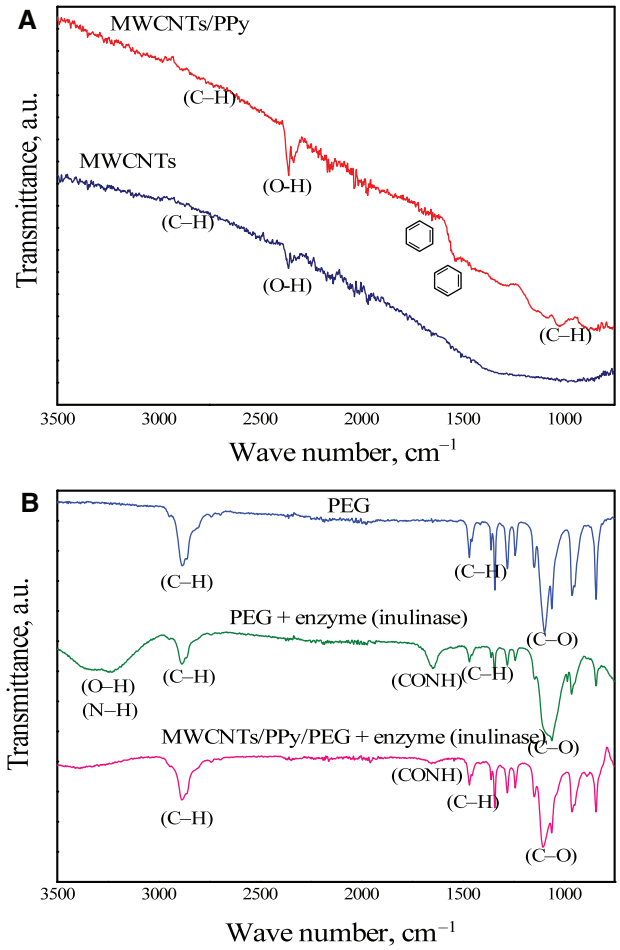

FIGURE 3 FTIR spectra: (A) Pristine *f*-MWCNTs and *f*-MWCNTs/PPy nanocomposite, which give featureless infrared spectra with just a handful of characteristic peaks. The reduction of the peak intensity at 2360 cm^{-1} in the spectrum of the MWCNTs/PPy nanocomposite in comparison to pristine MWCNTs suggests an efficient wrapping of the *f*-MWCNTs with PPy macromolecules. (B) (1) pristine PEG extract with characteristic band at 1096 cm^{-1}due to the C-O stretching, (2) aqueous PEG containing inulinase with two characteristic bands at 1649 and 1543 cm^{-1} emerging due to the amide group I and amide group II vibrations, respectively, originating from the protein and (3) the final *f*-MWCNTs/PPy/PEG–inulinase nanocomposite with characteristic amide peaks, that have lower intensity due to the lower concentration of inulinase in the immobilized preparation

the bands at 1130 cm^{-1} as well as in the region between 1023 and 1083 cm^{-1} are due to the in-plane vibrations of C–H bonds. In contrast, aforementioned bands do not appear in the spectrum of the *f*-MWCNTs/PPy nanocomposite, suggesting an effective wrapping of MWCNTs with the polymer and strong interaction between individual components of the nanocomposite. In the region between 2848 and 2882 cm^{-1}, there is characteristic band expected to appear due to the strong vibrations of C–H bond stretching; however, in this study this peak has not been found for both pristine *f*-MWCNTs and the *f*-MWCNTs/PPy nanocomposite. The most prominent band at ca. 2360 cm^{-1} corresponds to the O–H stretch emerging from a strongly hydrogen-bonding –COOH groups [58]. The reduction of the peak intensity at 2360 cm^{-1} in the spectrum of the MWCNTs/PPy nanocomposite in comparison to pristine MWCNTs suggests an efficient wrapping of the *f*-MWCNTs with PPy macromolecules.

Figure 3B corresponds to further steps of the *f*-MWCNTs/PPy/PEG-inulinase nanocomposite fabrication and presents the FTIR spectra of: (1) pristine PEG extract, (2) aqueous PEG containing inulinase and (3) the final *f*-MWCNTs/PPy/PEG–inulinase nanocomposite. The FTIR spectrum of PEG features the band at 2883 cm^{-1} emerging due to the aliphatic C-H stretching and peaks at 1466 cm^{-1} and 1341 cm^{-1} due to the C-H bending vibrations. The most prominent characteristic band in the PEG spectrum is observed at 1096 cm^{-1}due to the C-O stretching [58]. Significant spectral differences are seen in the PEG-inulinase system in comparison to pristine PEG. Thus, two characteristic bands at 1649 and 1543 cm^{-1} emerge due to the amide group I and amide group II vibrations, respectively, originating from the protein itself. Since the PEG-inulinase system retains residual water, the band at 3230 cm^{-1} could be assigned to the N-H and O-H stretching, or a mixture of both. Importantly, the characteristic amide peaks are also present in the final immobilized product–the MWCNT/PPy/PEG–inulinase. However, the bands have lower intensity due to the lower concentration of inulinase in the immobilized preparation [30,35,59,60]. This FTIR data unambiguously confirm that the enzyme becomes successfully incorporated into the target nanocomposite.

3.2 | Effect of enzyme concentration on the efficiency of immobilization

The effect of the enzymatic loading on immobilization yield and activity recovery is presented in Figure 4A. The loading of enzyme molecules onto nanoparticles is dependent on the amount of enzyme available for immobilization and the active surface area of the matrix. In this work, an efficient loading of inulinase onto the MWCNTs/polymer nanoparticles has been achieved; the loading varied between 57 and 345 μg of the deposited protein with the corresponding immobilization yields varying between 68 and 85%, respectively. High immobilization yield of ca. 85% achieved in this work is likely to be due to the high surface area of the nanocomposite, its porous structure, and high abundance of carboxylic functional groups [30,35]. The activity recovery (Figure 4A) was found to be proportional to the enzyme bonded to the support; it increased from 20.8 to 90.2% for the lowest and highest enzyme loadings, respectively. In this work, the quantity of the immobilized inulinase is two or three orders of

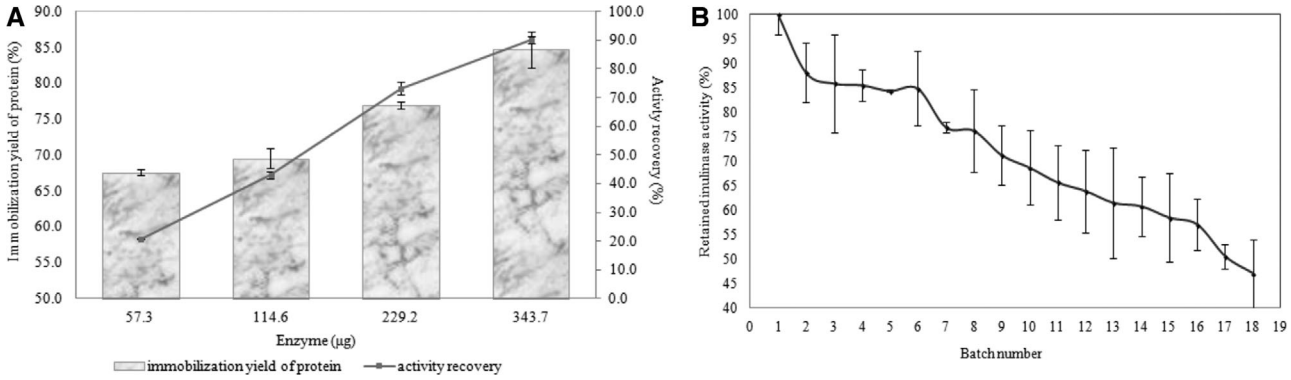

FIGURE 4 (A) The effect of the enzymatic loading on immobilization yield and activity. The loading of the enzyme varied between 57 and 345 μg with immobilization yields varying between 68 and 85%, respectively. The activity recovery increased from 20.8 to 90.2% for the lowest and highest enzyme loadings, respectively. (B) Operational stability of immobilized inulinase in batch operation mode. The MWCNT-inulinase composite retained 50% of its initial activity after 18 cycles

TABLE 1 Comparison of support-to-enzyme weight ratio, immobilization yield and catalytic activity of the present work with the published data

Publication	Immobilized preparation	Immobilization method	Support-to-enzyme weight ratio	Immobilization yield (%)	Catalytic activity (U/g)	"Normalised" Catalytic activity (U/g pure enzyme)
This work	Inulinase on *f*-MWCNT	Mixed non-covalent and covalent bonding	58:1	85.0	10.8	613.0
Costa et al., 2001	Catalase on alumina	Glutaraldehyde crosslinking (covalent bonding)	25:1	36.9	2190.0	54 750.0
Mubarak et al., 2014	Cellulase on MWCNT	Physical adsorption	1:1	97.6	0.98	0.98
Ahmad & Khare, 2018	Cellulase on MWCNT	Carbodiimide coupling (covalent bonding)	12:1	85.0	19.9	238.8
Gómez et al., 2005	β-glycosidase on MWCNT	Electrostatic interactions	1.6:1	/	400.0	640.0
Pavlidis et al., 2010	Lipase on *f*-MWCNT	Physical adsorption	10:1	53.9	/	539.0
Basso et al., 2010	Inulinase on amino Sepabeads	Amino: glutaraldehyde crosslinking	/	76.0	300.0	/
Basso et al., 2010	Inulinase on epoxy Sepabeads	Epoxy: nucleophilic attack	/	75.0	204.0	/
Singh & Chauhan, 2019	Inulinase on amino ($+NH_2$) MWCNT	Glutaraldehyde crosslinking	1.8:1	84.9	88.6	161.0
Singh et al., 2019	Inulinase on 3-aminopropyl-triethoxylane MWCNT	Covalent bond	3.3:1	74.4	9.0	29.7

magnitude smaller than the total mass of the nanocomposite. For example, even the highest loaded amount of 345 μg of the protein is very small compared to the 20 mg of the total mass of the nanocomposite, corresponding to ca. 60:1 nanocomposite-to-inulinase weight ratio. Such ratio is due to the fact that the enzyme is delivered to the nanocomposite by PEG, whose large molecules saturate the composite's porous structure and thus inhibit further uptake of the enzyme. To put our result into perspective, we compared the immobilized preparation produced in our work to a selection of other supported enzymatic systems reported in literature. The result of this comparative exercise is presented in Table 1. Using silanized alumina support, Costa et al., (2001) [39] has achieved the loading of 200 mg of the catalase onto 5 g of the support, corresponding to 25:1 support-to-catalase weight ratio. Mubarak et al., (2014) [14] have reported optimal enzyme loading of 1 mg of the enzyme to 1 mg support, while Gomez et al., (2005) [40] reported the highest enzyme load of 630 μg/mg support for the β-glycosidase immobilized on MWCNT corresponding to 1.6:1 support-to-enzyme ratio. Ahmad & Khare, (2018) [37] have achieved 85% immobilization efficiency of cellulase onto MWCNT. In contrast, Pavlidis et al., (2010) [18] have attained higher immobilization yield of 53.9% by using lower initial lipase

concentration, i.e. 10:1 support-to-enzyme ratio, rather than 1.6:1 support-to-enzyme ratio, when 40.6% immobilization yield was achieved. Good immobilization yield of 75 and 76% was achieved when inulinase was covalently immobilized on epoxy and amino Sepabeads via direct nucleophilic attack of ε-amino groups of lysine to the epoxy group or crosslinking by glutaraldehyde [61] using 77 U per gram wet polymer. The most recent studies [3,23] show that crosslinking and immobilizing the inulinase by glutaraldehyde on MWCNT significantly increase the immobilization yield from 60.7 to 84.9% but not the recovered activity, which remained around 74%. The authors used lower support-to-enzyme weight ratio when they achieved higher immobilization yield.

3.3 | Operational and storage stability of immobilized inulinase enzyme

To be economically viable, industrial enzymatic systems must be capable of retaining high catalytic activity after multiple uses. This goal can be achieved by attaching enzymes to solid supports; these immobilized catalysts can be recovered from reaction media and reused several times. The examination of operational stability in laboratory settings allows determining feasibility of industrial application of immobilized preparation. The results of operational stability evaluation of the inulinase immobilized on *f*-MWCNT/PPy composite are shown in Figure 4B. From Figure 4B, it can be seen that the activity of the immobilized inulinase gradually decreased after each cycle. The reason for this activity decline might be related to weakly bonded inulinase being detached and washed away from the CNT or its deactivation during the process. Nevertheless, the MWCNT-inulinase composite retained 50% of its initial activity after eighteen cycles. Our result compares quite favourably to the published data. For example, Zhu and Sun, 2012 [37] immobilized lipase on glutaraldehyde-activated nanofibrous membranes which retained activity of 69% after the tenth cycle. Ahmad and Khare, 2018 [60] were able to reuse their immobilized preparation ten times. Mubarak et al., [30] used MWCNT for cellulase immobilization which lost almost 50% of its initial activity at the sixth cycle; Pavlidis et al., [35] observed 10% decrease in enzymatic activity just after the fourth cycle of reuse. When inulinase was immobilized on 3-aminopropyltriethoxysilane *f*-MWCNTs, only 28% of the initial activity was preserved after the tenth consecutive batch cycle [3], but when the immobilization technique was improved by the same authors by adding cross-linking step with glutaraldehyde, the operational stability of the immobilization preparation has reached upto impressive 43 cycles. The immobilized enzyme of our preparation preserved 50% of its initial activity after 6 months of storage. Our findings are a promising result for potential use of this composite in industrial application.

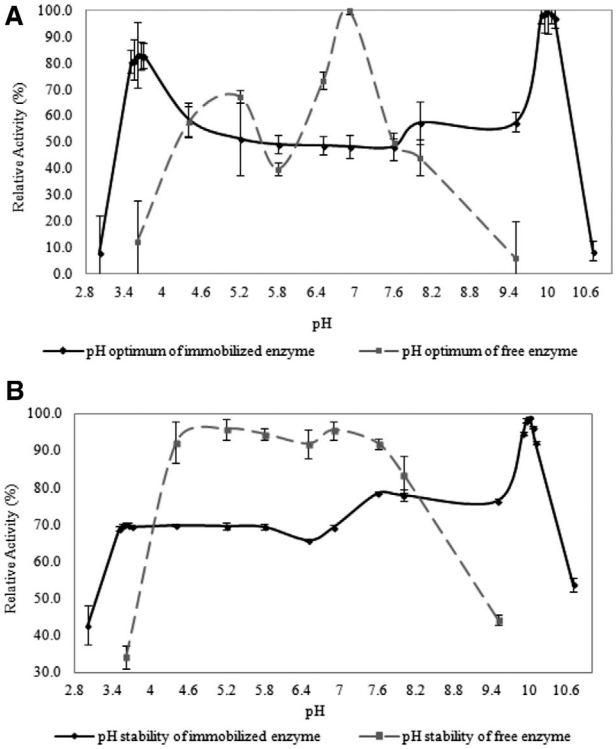

FIGURE 5 Effect of pH on free and immobilized inulinase: (A) pH optimum; (B) pH stability. The activity and stability of free and immobilized enzyme has been evaluated under the same conditions in a wide range of pH (3.0–10.7). The pH profile of the free enzyme (partially purified in PEG phase) exhibits two peaks of optimal pH at 8 and 5.8, suggesting that the inulinase is present in two multiple forms. pH profile for the partially purified immobilized inulinase on the *f*-MWCNT showed two pH optimums at 3.6 and 10. The free form of inulinase remained stable in the pH range between 4.6 and 7.6 retaining 96% of its initial activity after 2 hours of incubation, whereas the immobilized protein was stable at pH 10 preserving 99% of its initial activity

3.4 | Effect of pH on immobilized inulinase activity and stability

The normalized activity and stability of free and immobilized enzyme calculated for the same amount of enzyme has been evaluated under the same conditions in a wide range of pH (3.0–10.7); the results are shown in the Figure 5A and B. As reported in our previous study [46], the pH profile of the partially purified PEG phase free enzyme exhibits two peaks of optimal pH at 8 and 5.8, suggesting that the inulinase is present in two multiple forms. pH profile for the partially purified immobilized inulinase on the *f*-MWCNT prepared in this study also showed two pH optimums at 3.6 and 10 with the corresponding activity of 3.48 and 4.14 U/mg, respectively (Figure 5A). The immobilized enzyme exhibited activity throughout the whole range of studied pH. However, there was a dramatic decline of its activity at pH below 3.6 and above 10. The reduction of activity at low pH is

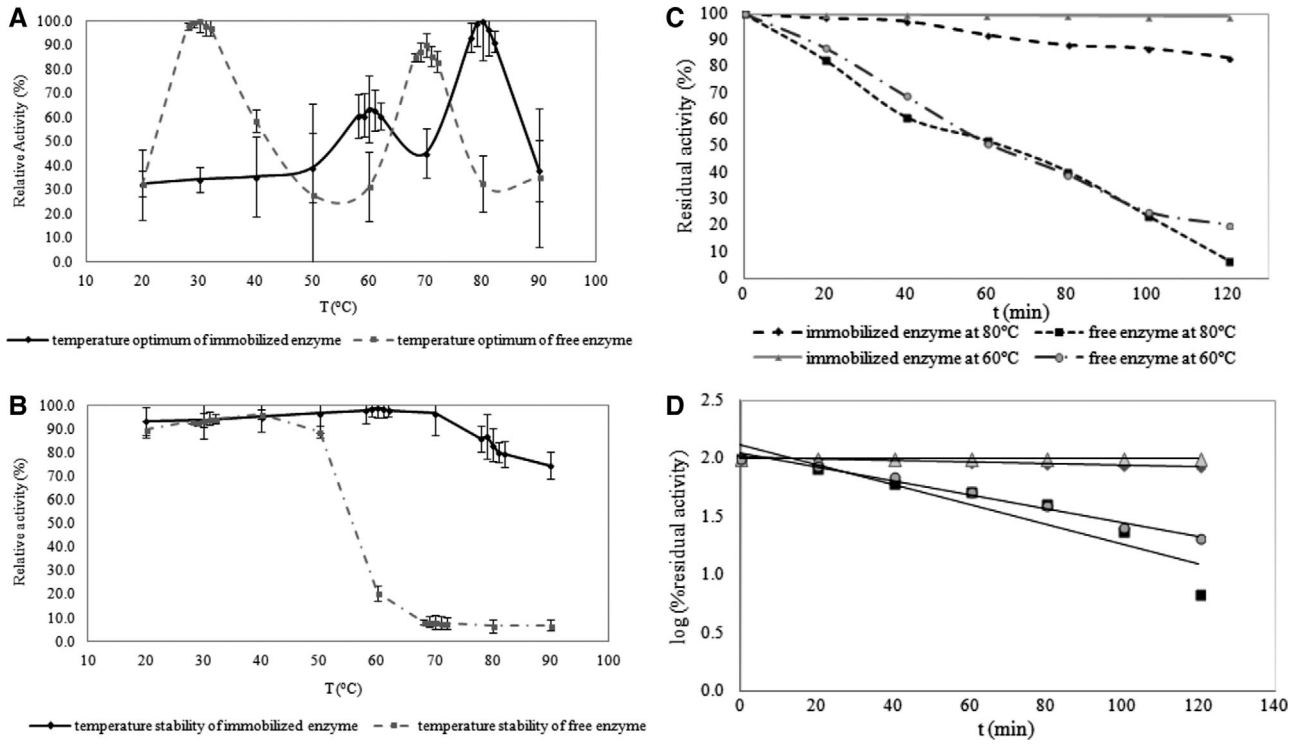

FIGURE 6 Effect of temperature on free and immobilized inulinase: (A) Temperature optimum; (B) Temperature stability, (C) Thermal inactivation kinetics study of free and immobilized inulinase at 60 and 80°C, (D) Arrhenius plot to calculate k_d. The effect of temperature on free and immobilized inulinase activity and stability was investigated in the temperature range of 20 to 90ºC. The profile of optimum temperature showed two peaks at 60 and 80ºC, compared to optimum temperature for free enzymes which was found to be at 30 and 70ºC. The MWCNT/PPy/PEG–inulinase at the optimum temperatures retained 99 and 83% of the initial enzymatic activity after 2 h of incubation. The $t_{1/2}$ of the immobilized inulinases at 60 and 80ºC were 288.8 and 16.5 h, respectively, while deactivation of the unsupported protein under the same conditions was 1.9 and 1.3 h, respectively

caused by the H^+ ions affecting the conformation of inulinase molecule and its net charge. Highly alkaline conditions are known to cause the distortion of enzyme's active center brought about by electrostatic repulsion and stretching of the protein molecule [30]. In comparison to the free form of inulinase, the pH of the optimal performance for the immobilized enzyme is shifted towards more extreme pH conditions (both alkaline and acidic). This is likely to be due to the presence of polyvalent ions in the immobilization matrix [62].

The free form of inulinase remained stable in the pH range between 4.6 and 7.6 retaining ca. 96% of its initial activity after 2 h of incubation (Figure 4B), whereas the immobilized protein was particularly stable at pH 10 preserving up to 99% of its initial activity. Under neutral and acidic conditions, the relative activity of the immobilized inulinase was found to be about 70%. It is proposed that the enhanced pH stability of the immobilized form of enzyme is improved by limiting undesired conformation changes in accordance with the multi-point attachment mechanism [37]. A case in point is the study by Gestrelius et al., 1973 [63] which examined micro environmental pH effects and found out that pH optimum for immobilized trypsin activity shifted 1.3 pH unit (to pH 9.6) and the pH optimum for immobilized glucose oxidase shifted 0.3 pH units to the alkaline side (to pH 6.9). Xu et al., 2016 [64] also reported pH shift in the alkaline range when lipase from *Aspergillus niger* was immobilized on SiO_2 nanoparticles.

3.5 | Effect of temperature on the immobilized inulinase activity and stability

The effect of temperature on free and immobilized inulinase activity and stability was investigated in the temperature range of 20 to 90ºC (Figure 6A and B). The profile of optimum temperature showed, as expected, two peaks at 60 and 80ºC with the normalized activity of 4.25 and 6.69 U/mg, respectively, compared to optimum temperature for free enzymes which was found to be at 30 and 70ºC, respectively. The shift towards higher temperatures observed for the immobilized form of inulinase can be explained by the requirement to achieve higher energy of activation, since the conformational mobility of enzymes, bonded to support, is generally reduced. In addition, the supported enzyme exhibits increased stability and resistance towards thermally induced denaturation [65].

In this work, stability of immobilized inulinase was dramatically increased in comparison to the free form of enzyme.

TABLE 2 Kinetic parameters for thermal inactivation of free and immobilized inulinases

	k_d	D value	$t_{1/2}$ (h)
Immobilized enzyme at 60ºC	0.00004	57 564.6	288.8
Immobilized enzyme at 80ºC	0.0007	3289.4	16.5
Free enzyme at 60ºC	0.006	383.7	1.9
Free enzyme at 80ºC	0.0086	267.7	1.3

Immobilized enzyme retained above 90% of its initial activity from 20 to 70ºC, after which the activity dropped to 75% at 90ºC during the period of 2 h of incubation. In contrast, the free enzyme retained above 90% from its initial activity from 20 to 50ºC, which followed an activity drop to 20% at 60ºC, and just 8% at 70ºC during the same period of time of incubation.

Furthermore, in Figure 6C the residual activity versus time of the immobilized and free form of the enzyme at optimum temperatures are presented, whereas the thermal stability was evaluated in terms of the rate constant of deactivation (k_d) derived as slopes of the plots of log residual activity versus time presented in Figure 6D. The results in Figure 6C showed that the free enzyme lost 50% of the activity after 1 h at 80ºC, while the immobilized enzyme retained more than 90% at the same temperature. At 60ºC, the free enzyme lost again 50% of its activity, but the immobilized enzyme retained almost 100% at the same conditions. Obtained results indicate that the free form inulinases show higher deactivation constants at 60 and 80ºC in contrast to the immobilized enzyme under the same conditions. Thus, the $t_{1/2}$ of the immobilized inulinases at 60 and 80ºC were 288.8 and 16.5 h, respectively, while deactivation of the unsupported protein under the same conditions was 1.9 and 1.3 h, respectively. The decimal reduction time was the highest for the immobilized enzyme at 60ºC and the lowest for the free enzyme at 80ºC. Full data of kinetic parameters for thermal inactivation of free and immobilized inulinases is given in Table 2. We link the increased thermal durability of the immobilized inulinase to a higher stability of the enzyme's structure immobilized on CNTs [60,66,67]. The enzymes with increased stability are more suitable for industrial applications [67].

This interpretation is supported by several published studies. Thus, Ghada et al., 2017 [67] reported that the half-lives and *D* values of inulinase after covalent immobilization indicated better thermal stability of the immobilized inulinase. Karimi et al., 2014b [26] have shown that the immobilization of endo-inulinase increases thermal optimum of the enzyme allowing the reaction to be conducted at higher temperatures. The high temperature regime of operation aids to prevent microbial contamination and allows better solubility of inulin as substrate. Zhu and Sun, 2012 [37] have reported the thermal optimum shifted towards higher temperature when lipase was immobilized on glutaraldehyde-activated nanofibrous membranes. Increased temperature optimum (70ºC) for the protease immobilized on chitosan nanoparticles was reported by Shojaei et al., 2017 [65]. Garlet et al., 2014 [24] have reported 50°C as an optimum temperature for the immobilized inulinase on CNTs, with the enzyme retaining 93% of its initial activity after 4 h of incubation. Yewale et al., 2013 [17] have established 60°C as an optimum temperature for the immobilized inulinase from *A. niger* NCIM 945 on chitosan and reported impressive 100% retention of the initial activity after 2 h of incubation.

3.6 | Kinetics studies

Kinetic parameters, K_m and V_m, of free and immobilized enzyme were calculated from by Lineweaver–Burk plot. Various amounts from 0.5 to 3.0% of substrate (inulin) were used to measure the initial rate of the reaction. Michaelis–Menten kinetics was observed for both the enzymes. For the free enzyme K_m was determined as 26 μM and V_{max} as 526 U/min, while for the immobilized enzyme K_m was found to be 5.71 μM and V_{max} decreased to 2.99 U/min. Generally, low values of K_m signify high affinity between the enzyme and the substrate. In this regard, the enzyme immobilized onto *f*-MWCNTs has better affinity towards the substrate, likely because of the high contact area of CNTs and an abundance of the carboxyl functional groups available for binding. Furthermore, the functionalization of CNTs with PPy and PEG helps to maximize the total surface area by spacing out individual components and makes the immobilized enzyme easily accessible for the substrate attachment [44,68]. However, the maximal rate was 175 fold decreased. This change may occur due to the inactivation of the enzyme along with the bonding or by secluding the active centers [69]. The combination of a lower maximal rate and higher K_m was observed in lipase immobilized on amino-f-MWCNT by Verma et al., 2013 [69], as well as in immobilized lipase on nanofibrous membranes by Zhu & Sun, 2012 [37]. The latter found increase in their K_m value compared to the free enzyme.

4 | CONCLUDING REMARKS

In this research two multiple forms of inulinases, extracted in PEG by ATPS method, were succesfully immobilized on *f*-MWCNT with PPy via mixed attachment of the enzyme and physical wraping of PEG around nanoparticles. The morphology and chemical composition of pristine and immobilized MWCNT has been proven using techniques such as SEM and FTIR. The optimal enzyme load was found to be 344 μg which gave immobilization yield of protein of 85% and retained 50% of its initial activity up until the eighteenth cycle. The immobilized preparation had two pH optima at 3.6 and 10.0 and was stable at alkaline conditions retaining 99% of its initial

activity after 2 h of incubation. The temperature optimum was at 60 and 80ºC and the $t_{1/2}$ at these optima were 231 and 99 min, respectively, indicating that produced catalyst had enhanced thermal stability. *f*-MWCNT were found to be an excellent support for the enzyme immobilization directly from PEG material. The prepared catalyst can be reused several times, reducing the demand for the enzyme and improving the economy of the process by avoiding the ultrafiltration step from PEG. For industrial application CNT are 3.2 times more costly than chitosan beads, but they are preferred carriers for their balancing key aspects that determine the efficiency of the biocatalysts, such as large surface area, high mechanical properties and minimum diffusion limitation.

ACKNOWLEDGMENTS

This work has been funded by National Science Fund of Bulgaria under Project DN 06/11. Dr Aliaksandr Baidak is supported by the Dalton Fellowship provided through the Dalton Nuclear Institute, the University of Manchester.

CONFLICT OF INTEREST

The authors have declared no conflict of interest.

ORCID

Albert Krastanov https://orcid.org/0000-0003-2794-1655

REFERENCES

1. Neagu, C., Bahrim, G., Inulinases - a versatile tool for biotechnology. *Innovative Rom. Food Biotechnol.* 2011, *9*, 1–11.
2. Treichel, H., Oliveira, D. d., Lerin, L., Astolfi, V. et al., A review on the production and partial characterization of microbial inulinases. *Global J. Biochem.* 2012, *3*, 1–7.
3. Singh, R. S., Chauhan, K., Kennedy, J. F., Fructose production from inulin using fungal inulinase immobilized on 3-aminopropyltriethoxysilane functionalized multiwalled carbon nanotubes. *Int. J. Biol. Macromol.* 2019, *125*, 41–52.
4. Ricca, E., Calabrò, V., Curcio, S., Iorio, G., Fructose production by chicory inulin enzymatic hydrolysis: a kinetic study and reaction mechanism. *Process Biochem.* 2009, *44*, 466–470.
5. Ricca, E., Calabro, V., Curcio, S., Iorio, G., The state of the art in the production of fructose from inulin enzymatic hydrolysis. *Crit. Rev. Biotechnol.* 2007, *27*, 129–145.
6. Singh, R. S., Singh, R. P., Production of fructooligosaccharides from Inulin by endoinulinases and their prebiotic potential. *Food Technol. Biotechnol.* 2010, *48*, 435–450.
7. Picazo, B., Flores-Gallegos, A. C., Muñiz-Márquez, D. B., Flores-Maltos, A. et al., Enzymes for fructooligosaccharides production: achievements and opportunities, in: Kuddus, M. (Ed.), *Enzymes in Food Biotechnology. Production, Applications, and Future Prospects* Academic Press 2019, pp. 303–320.
8. Apolinario, A. C., de Lima Damasceno, B. P., de Macedo Beltrao, N. E., Pessoa, A. et al., Inulin-type fructans: a review on different aspects of biochemical and pharmaceutical technology. *Carbohydr. Polym.* 2014, *101*, 368–378.
9. Wang, Y. Z., Zou, S. M., He, M. L., Wang, C. H., Bioethanol production from the dry powder of Jerusalem artichoke tubers by recombinant *Saccharomyces cerevisiae* in simultaneous saccharification and fermentation. *J. Ind. Microbiol. Biotechnol.* 2015, *42*, 543–551.
10. Liu, X. Y., Chi, Z., Liu, G. L., Wang, F. et al., Inulin hydrolysis and citric acid production from inulin using the surface-engineered *Yarrowia lipolytica* displaying inulinase. *Metab. Eng.* 2010, *12*, 469–476.
11. Chi, Z. M., Zhang, T., Cao, T. S., Liu, X. Y. et al., Biotechnological potential of inulin for bioprocesses. *Bioresour. Technol.* 2011, *102*, 4295–4303.
12. Datta, S., Christena, L. R., Rajaram, Y. R., Enzyme immobilization: an overview on techniques and support materials. *3 Biotech.* 2013, *3*, 1–9.
13. Brena, B. M., Batista-Viera, F., Immobilization of Enzymes, in: Guisan, J. M. (Ed.), *Methods in Biotechnology: Immobilization of Enzymes and Cells*, Humana Press Inc, Totowa, NJ 2006, p. 450.
14. Sheldon, R. A., Enzyme immobilization: The quest for optimum performance. *Adv. Synth. Catal.* 2007, *349*, 1289–1307.
15. Cantone, S., Ferrario, V., Corici, L., Ebert, C. et al., Efficient immobilisation of industrial biocatalysts: criteria and constraints for the selection of organic polymeric carriers and immobilisation methods. *Chem. Soc. Rev.* 2013, *42*, 6262–6276.
16. Kim, C. H., Rhee, S. K., Fructose production from Jerusalem artichoke by inulinase immobilized on chitin. *Biotechnol. Lett.* 1989, *11*, 201–206.
17. Yewale, T., Singhal, R. S., Vaidya, A. A., Immobilization of inulinase from *Aspergillus niger* NCIM 945 on chitosan and its application in continuous inulin hydrolysis. *Biocatal. Agric. Biotechnol.* 2013, *2*, 96–101.
18. Danial, N. E., Elnashar, M. M. M., Awad, E. A. G., Immobilized inulinase on grafted alginate beads prepared by the one-step and the two-steps methods. *Ind. Eng. Chem. Res.* 2010, *49*, 3120–3125.
19. Missau, J., Scheid, A. J., Foletto, E. L., Jahn, S. L. et al., Immobilization of commercial inulinase on alginate chitosan beads. *Sustainable Chem. Processes.* 2014, *2*.
20. Singh, R. S., Singh, R. P., Kennedy, J. F., Immobilization of yeast inulinase on chitosan beads for the hydrolysis of inulin in a batch system. *Int. J. Biol. Macromol.* 2017, *95*, 87–93.
21. Silva, M. F., Rigo, D., Mossi, V., Dallago, R. M. et al., Evaluation of enzymatic activity of commercial inulinase from *Aspergillus niger* immobilized in polyurethane foam. *Food Bioprod. Process.* 2013, *91*, 54–59.
22. Fernandes, P., Fonseca, L. P., Cattorini, S., Carvalho, F. et al., *XVIth International Conference on Bioencapsulation*, Dublin, Ireland 2008, P50.
23. Singh, R. S., Chauhan, K., Immobilization of inulinase on aminated multiwalled carbon nanotubes by glutaraldehyde cross-linking for the production of fructose. *Catal. Lett.* 2019.
24. Garlet, T. B., Weber, C. T., Klaic, R., Foletto, E. L. et al., Carbon nanotubes as supports for inulinase immobilization. *Molecules* 2014, *19*, 14615–14624.
25. Karimi, M., Chaudhury, I., Jianjun, C., Safari, M. et al., Immobilization of endo-inulinase on non-porous amino functionalized silica nanoparticles. *J. Mol. Catal. B Enzym.* 2014, *104*, 48–55.

26. Karimi, M., Habibi-Rezaei, M., Safari, M., Moosavi-Movahedi, A. A. et al., Immobilization of endo-inulinase on poly-d-lysine coated $CaCO_3$ micro-particles. *Food Res. Int.* 2014, *66*, 485–492.
27. Torabizadeh, H., Mahmoudi, A., Inulin hydrolysis by inulinase immobilized covalently on magnetic nanoparticles prepared with wheat gluten hydrolysates. *Biotechnol Rep (Amst).* 2018, *17*, 97–103.
28. Paripoorani, K. S., Ashwin, G., Vengatapriya, P., Ranjitha, V. et al., Insolubilization of inulinase on magnetite chitosan microparticles, an easily recoverable and reusable support. *J. Mol. Catal. B Enzym.* 2015, *113*, 47–55.
29. Prato, M., Kostarelos, K., Bianco, A., Functionalized carbon nanotubes in drug design and discovery. *Acc. Chem. Res.* 2008, *41*, 60–68.
30. Mubarak, N. M., Wong, J. R., Tan, K. W., Sahu, J. N. et al., Immobilization of cellulase enzyme on functionalized multiwall carbon nanotubes. *J. Mol. Catal. B Enzym.* 2014, *107*, 124–131.
31. Feng, W., Ji, P., Enzymes immobilized on carbon nanotubes. *Biotechnol. Adv.* 2011, *29*, 889–895.
32. Jia, H., Zhu, G., Wang, P., Catalytic behaviors of enzymes attached to nanoparticles: the effect of particle mobility. *Biotechnol. Bioeng.* 2003, *84*, 406–414.
33. Wang, W., Li, Z., Wang, D. I. C., *Nanotech*, Washington, DC 2009, pp. 337–339.
34. Meshram, B. H., Kondawar, S. B., Mahajan, A. P., Mahore, R. P., Burghate, D. K., Urease immobilized polypyrrole/multi-walled carbon nanotubes composite biosensor for heavy metal ions detection. *J. Chin. Adv. Mater. Soc.* 2014, *2*, 223–235.
35. Pavlidis, I. V., Tsoufis, T., Enotiadis, A., Gournis, D., Stamatis, H., Functionalized multi-wall carbon nanotubes for lipase immobilization. *Adv. Eng. Mater.* 2010, *12*, B179-B183.
36. Kim, B. J., Kang, B. K., Bahk, Y. Y., Yoo, K. H., Lim, K. J., Immobilization of horseradish peroxidase on multi-walled carbon nanotubes and its enzymatic stability. *Curr. Appl Phys.* 2009, *9*, e263-e265.
37. Zhu, J., Sun, G., Lipase immobilization on glutaraldehyde-activated nanofibrous membranes for improved enzyme stabilities and activities. *React. Funct. Polym.* 2012, *72*, 839–845.
38. Tasis, D., Tagmatarchis, N., Bianco, A., Prato, M., Chemistry of carbon nanotubes. *Chem. Rev.* 2006, *106*, 1105–1136.
39. Subbenaik, C., Sanmathi Physical and chemical nature of nanoparticles. 2016, 15–27.
40. Nagaraju, K., Reddy, R., Reddy, N., A review on protein functionalized carbon nanotubes. *J. Appl. Biomater. Funct. Mater.* 2015, *13*, e301–312.
41. Sahoo, N. G., Rana, S., Cho, J. W., Li, L., Chan, S. H., Polymer nanocomposites based on functionalized carbon nanotubes. *Prog. Polym. Sci.* 2010, *35*, 837–867.
42. Fan, J., Wan, M., Zhu, D., Chang, B. et al., Synthesis, characterizations and physical properties of carbon nanotubes coated by conducting polypyrrole. *J. Appl. Polym. Sci.* 1999, *74*, 2605–2610.
43. Jain, S., Toxicity issues related to biomedical applications of carbon nanotubes. *J. Nanomed. Nanotechnol.* 2012, *03*.
44. Ateh, D. D., Navsaria, H. A., Vadgama, P., Polypyrrole-based conducting polymers and interactions with biological tissues. *J. R. Soc. Interface.* 2006, *3*, 741–752.
45. Kim, B. C., Lee, I., Kwon, S. J., Wee, Y. et al., Fabrication of enzyme-based coatings on intact multi-walled carbon nanotubes as highly effective electrodes in biofuel cells. *Sci. Rep.* 2017, *7*, 40202.
46. Temkov, M., Strinska, H., Dobrev, G., Velickova, E. et al., Purification of bacterial inulinase in aqueous two-phase systems. *Eng. Life Sci.* 2018, *18*, 840–850.
47. Eisazadeh, H., Studying the characteristics of polypyrrole and its composites. *World J. Chem.* 2007, *2*, 67–74.
48. Shim, M., Wong Shi Kam, N. J., Chen, R., Li, Y., Dai, H., Functionalization of carbon nanotubes for biocompatibility and biomolecular recognition. *Nano Lett.* 2002, *2*, 285–288
49. Villalonga, R., Villalonga, M. L., Díez, P., Pingarrón, J. M., Decorating carbon nanotubes with polyethylene glycol-coated magnetic nanoparticles for implementing highly sensitive enzyme biosensors. *J. Mater. Chem.* 2011, *21*, 12858.
50. Fujigaya, T., Nakashima, N., Non-covalent polymer wrapping of carbon nanotubes and the role of wrapped polymers as functional dispersants. *Sci. Technol. Adv. Mater.* 2015, *16*, 024802.
51. Balint, R., Cassidy, N. J., Cartmell, S. H., Conductive polymers: towards a smart biomaterial for tissue engineering. *Acta Biomater.* 2014, *10*, 2341–2353.
52. Gavrailov, S., Ivanova, V., Isolation and characteristics of a thermophilic *Bacillus* strain, producer of inulinase. *J. BioSci. Biotech.* 2014, 83–94.
53. Bradford, M. M., A rapid and sensitive method for the quantitation of microgram quantities of protein utilizing the principle of protein-dye binding. *Anal. Biochem.* 1976, *72*, 248–254.
54. Lever, M., A new reaction for colorimetric determination of carbohydrates. *Analitical Biochemistry.* 1972, *47*, 273–279.
55. Zhang, H., Guo, H., Deng, X., Gu, P. et al., Functionalization of multi-walled carbon nanotubes via surface unpaired electrons. *Nanotechnology.* 2010, *21*, 85706.
56. Okan, B. S., Zanjani, J. S. M., Letofsky-Papst, I., Cebeci, F. Ç., Menceloglu, Y. Z., Morphology-controllable synthesis and characterization of carbon nanotube/polypyrrole composites and their hydrogen storage capacities. *Mater. Chem. Phys.* 2015, *167*, 171–180.
57. Canobre, S. C., Xavier, F. F. S., Fagundes, W. S., de Freitas, A. C., Amaral, F. A., Performance of the chemical and electrochemical composites of PPy/CNT as electrodes in type I supercapacitors. *J. Nanomater.* 2015, *2015*, 1–13.
58. Shameli, K., Ahmad, M. B., Jazayeri, S. D., Sedaghat, S. et al., Synthesis and characterization of polyethylene glycol mediated silver nanoparticles by the green method. *Int. J. Mol. Sci.* 2012, *13*, 6639–6650.
59. Zhang, D., Hegab, H. E., Lvov, Y., Dale Snow, L., Palmer, J., Immobilization of cellulase on a silica gel substrate modified using a 3-APTES self-assembled monolayer. *SpringerPlus.* 2016, *5*, 48.
60. Ahmad, R., Khare, S. K., Immobilization of *Aspergillus niger* cellulase on multiwall carbon nanotubes for cellulose hydrolysis. *Bioresour. Technol.* 2018, *252*, 72–75.
61. Basso, A., Spizzo, P., Ferrario, V., Knapic, L. et al., Endo- and exo-inulinases: enzyme-substrate interaction and rational Immobilization. *Biotechnol. Prog.* 2010, *26*, 397–405.
62. Costa, S. A., Tzanov, T., Paar, A., Gudelj, M. et al., Immobilization of catalases from Bacillus SF on alumina for the treatment of textile bleaching effluents. *Enzyme Microb. Technol.* 2001, *28*, 815–819.
63. Gestrelius, S., Mattiasson, B., Mosbach, K., On the regulation of the activity of immobilized enzymes. *Eur. J. Biochem.* 1973, *36*, 89–96.

64. Xu, L., Ke, C., Huang, Y., Yan, Y., Immobilized *Aspergillus niger* lipase with SiO_2 nanoparticles in sol-gel materials. *Catalysts.* 2016, *6*, 149.
65. Shojaei, F., Homaei, A., Taherizadeh, M. R., Kamrani, E., Characterization of biosynthesized chitosan nanoparticles from *Penaeus vannamei* for the immobilization of *P. vannamei* protease: An eco-friendly nanobiocatalyst. *Int. J. Food Prop.* 2017, 1–11.
66. Khan, M., Husain, Q., Bushra, R., Immobilization of b-galactosidase on surface modified cobalt/multiwalled carbon nanotube nanocomposite improves enzyme stability and resistance to inhibitor. *Int. J. Biol. Macromol.* 2017, *105*, 693–701.
67. Awad, G. E. A., Wehaidy, H. R., Abd El Aty, A. A., Hassan, M. E., A novel alginate–CMC gel beads for efficient covalent inulinase immobilization. *Colloid Polym. Sci.* 2017, *295*, 495–506.
68. Manta, C., Ferraz, N., Betancor, L., Antunes, G. et al., Polyethylene glycol as a spacer for solid-phase enzyme immobilization. *Enzyme Microb. Technol.* 2003, *33*, 890–898.
69. Verma, M. L., Naebe, M., Barrow, C. J., Puri, M., Enzyme immobilisation on amino-functionalised multi-walled carbon nanotubes. Structural and biocatalytic characterisation. *PLoS One.* 2013, *8*.

How to cite this article: Temkov M, Petrovski A, Gjorgieva E, et al. Inulinase immobilization on polyethylene glycol/polypyrrole multiwall carbon nanotubes producing a catalyst with enhanced thermal and operational stability. *Eng Life Sci*. 2019;19:617–630. https://doi.org/10.1002/elsc.201900021